

Research Article

Experimental Investigation on Thermal Behaviors of Nanosilicon Carbide/Kenaf/Polymer Composite

R. Ganesh,¹ P. Anand ¹ and Wubishet Degife Mammo ²

¹Vel Tech Rangarajan Dr. Sagunthala R&D Institute of Science and Technology, Chennai, India

²Mechanical Engineering Department, Wollo University, Kombolcha Institute of Technology, Kombolcha, South Wollo-208, Amhara, Ethiopia

Correspondence should be addressed to P. Anand; p.anand@ymail.com and Wubishet Degife Mammo; wubishetdegife7@gmail.com

Received 11 March 2022; Revised 7 April 2022; Accepted 21 April 2022; Published 6 May 2022

Academic Editor: S.K. Khadheer Pasha

Copyright © 2022 R. Ganesh et al. This is an open access article distributed under the Creative Commons Attribution License, which permits unrestricted use, distribution, and reproduction in any medium, provided the original work is properly cited.

Over the last few years, natural fiber-based hybrid polymers have been widely used to increase the biodegradability and cost-effectiveness of the products in many industrial applications, such as automobile construction industries. Adding filler materials provides enhanced wear properties and thermal behaviors of composites. Kenaf fiber has better strength and stiffness, and it has been used as reinforcement in polymer composites. Silicon carbide as filler material in composites modifies the mechanical properties and thermal behaviors. The present research analyzes the thermal characteristics of silicon carbide/kenaf fiber-reinforced epoxy composites with various weight percentages. Six different composite specimens were fabricated at varying weight percentages of silicon carbide. The specimens were subjected to various thermal tests, such as heat deflection temperature (HDT), coefficient of thermal expansion (CTE), thermal conductivity (TC), thermogravimetric analysis (TGA), and differential scanning calorimetry (DSC). The findings could serve to expand the range of application for SiC/kenaf fiber-reinforced composite, which may have better thermal stability, better performance, and lower thermal expansion than the other regularly used natural fiber-reinforced composites.

1. Introduction

Adding various fillers into polymers enhances the properties of polymers. As a result, composites use polymers to a large extent. Fillers might lower the cost of composite materials with desirable mechanical and thermal properties [1]. Automotive, aerospace, construction, and marine sectors all employ composites made of epoxy as the matrix material in load-bearing applications. They have strong mechanical qualities, high specific strength, and extreme adhesiveness and are highly resistant to heat and solvents [2]. Natural fibers provide a number of advantages when used as a reinforcing medium. The majority of them are biodegradable, making disposal easier and more environmentally beneficial. Because of their lightweight and specific strength qualities, they are helpful in structural applications [3, 4]. Natural fiber manufacturing is rising globally as the product base

expands. Each year, natural fiber-based products replace synthetic fibers and high-energy-consuming items [5]; despite the numerous advantages provided by natural fiber composite materials, they have downsides, such as imperfect interfacial adhesion between constituents, moisture absorption, and erratic thermal behavior [6]. The mechanical characteristics of epoxy composites made of natural fiber reinforcement have been improved due to chemical treatments. Hemicelluloses and pectin compounds were removed from the fibers by surface treatments. Chemically treated fibers had an uneven surface and a larger effective surface area, allowing for greater fiber-matrix interaction [7]. Woven natural fiber fabric could be a possible reinforcing material for environmental-friendly polymers, according to Nurul Fazita et al. Synthetic fiber usage was limited by the introduction of natural fibers in the composites [8]. According to Akil et al., the usage of kenaf fiber-based polymers in

the field of architecture and structural applications is very feasible because of their lightweight and low cost [9, 10]. Malik et al. noted that the kenaf fiber is a powerful natural fiber and may be used in composites to replace glass fibers. It outperformed glass fibers in tensile strength and modulus. The filler materials also increased the performance of KFRCs, if reducing the size of filler material used in the composites [11]. A variety of methods are used to produce composite materials, each of which is appropriate for a certain material. The type and volume of matrix or fiber utilized determine the fabrication method's performance [12]. The addition of silicon carbide fillers to natural fiber-reinforced polymers improves their mechanical performance. The granule size and filling percentage of SiC granules are two significant characteristics to address. Smaller size granules are distributed in resins better than those of larger size granules [13]. The hybridized banana/kenaf fibers composites improved the mechanical characteristics of banana/kenaf fiber hybrid composites. The mechanical characteristics of three distinct types of fiber composites were examined by Alavuddeen et al. [14]. The effect on the properties of the hybrids made of glass/sisal fiber and fillers was explored by Arpitha et al. The use of E-glass with SiC particles could help to eliminate voids and improve physical qualities. The effect of the filler might improve the flexural characteristics of the material [15]. Silicon carbide (SiC) is used in composites to improve thermal conductivity. Adding SiC fillers into epoxides enhances their heat conductivity [16]. Because polymers have low thermal conductivity, fillers such as zinc oxide, alumina, aluminum nitride, mica, glass fiber, silicon carbides, and boron nitride have been used to enhance thermal conductivity and electrical resistance. Zinc oxide, aluminum nitride, mica, and glass fiber particles are among the other materials used [17]. The thermal firmness of polymers made of biofibers could inflict constraints in situations where the organic structure of the fiber is degraded. In theory, temperature impacts not just the structure but also the majority of attributes of natural fiber-reinforced polymers. The study of the composite basic thermogravimetric analysis demands a full understanding of these phenomena [18]. As a function of time and temperature, the DSC determines material transitions. The thermal phase change of the composites is shown by the endothermic (heat absorption) and exothermic (heat release) peaks and magnitudes [19, 20]. The sample shape and size, the temperature ramp, and the kind of environment can all have an impact on the results gathered by the DSC study. The thermal stability of natural fiber and hybrid composites was investigated by several authors using the DSC method [21, 22].

In this present work, the kenaf fiber-reinforced epoxy polymers were fabricated employing a compression molding process accompanied by varying percentages (2%, 4%, 6%, 8%, and 10%) of silicon carbide filler materials. Five silicon carbide/kenaf fiber-reinforced hybrid composites and a reference kenaf fiber-reinforced composites are subjected to various thermal tests, such as thermal conductivity (TC), heat deflection temperature (HDT), coefficient of thermal expansion (CTE), thermogravimetric analysis (TGA), and differential scanning calorimetry analysis (DSC). The test results were analyzed and compared.

TABLE 1: Properties of constituents of hybrid polymers.

Property	Epoxy resin	Kenaf fiber	Silicon carbide
Density in g/cm^3	1.14	1.2-1.6	3.2
Areal density in GSM	—	380	—
Thickness in mm	—	1.25	—
Structure of fabric	—	Plain woven	—
Tensile strength in MPa	73.3	220-930	—
Percentage of elongation	4.5	1.5-2.7%	—
Elastic modulus in GPa	3470	15-53	410
Thermal conductivity in W/mK	0.2	0.206	120

2. Materials

Kenaf fiber of density $1.2-1.6 \text{ g/cm}^3$ as a woven fabric was purchased from M/s. Go Green Products Pvt. Ltd., Tamil Nadu, India. Kenaf fiber fabric's mesh size is eight openings per inch with mesh no. 8 (2.38 mm), whereas silicon carbide filler size of $25 \mu\text{m}$ was supplied by Vazirbun Trading Pvt. Ltd., India. Hardener (HY951) and epoxy (LY556) were provided by SM composites, Chennai, India. The properties of kenaf fiber, SiC, and epoxy resins are listed in Table 1 [23–25]. Figure 1 shows the work methodology.

3. Fabrication Process

A 6 percent NaOH alkali treatment for kenaf fiber was chosen. Furthermore, the kenaf fiber was kept for 10 hours in 6% of NaOH and dried [26]. The composites were developed using hand layup preceding just before the compression molding process. A mold of $250 \text{ mm} \times 250 \text{ mm}$ stainless steel was used. A 10:1 ratio was utilized to mix resin and hardener. By weight, the fiber and matrix are at a 2:3 ratio. Fiber orientation in the layer is +90, -90. SiC fillers were added in composite laminate in terms of various volume percentages. Trial and error methods were used to obtain the optimum fiber volume fraction of the prepared composites with various stacking sequences. The optimal fiber volume fraction ranges between 0.35 and 0.42. Five composite laminates (2%, 4%, 6%, 8%, and 10% volume of composites, respectively) and one reference laminate with no fillers were fabricated. Uniform dispersion and the amount of filler particles added in the composites are the most important factor to attain exceptional thermal behavior for composites [27]. The silicon carbide fillers are assorted with the epoxy using a motorized stirrer for about 3 minutes to attain proper dispersion. The kenaf fiber was placed in the mold, and epoxy resins were poured onto the fiber and roller to spread the resin all over the fiber to be wet. Once the hand layup process was done, the mold was kept in the compression molding machine. The hot die, as same as of mold, was pressed against the mold with the force of 20 KN. Hot die temperature of 200°C helped in the curing process of composite laminates for an hour, and the postcuring process was carried

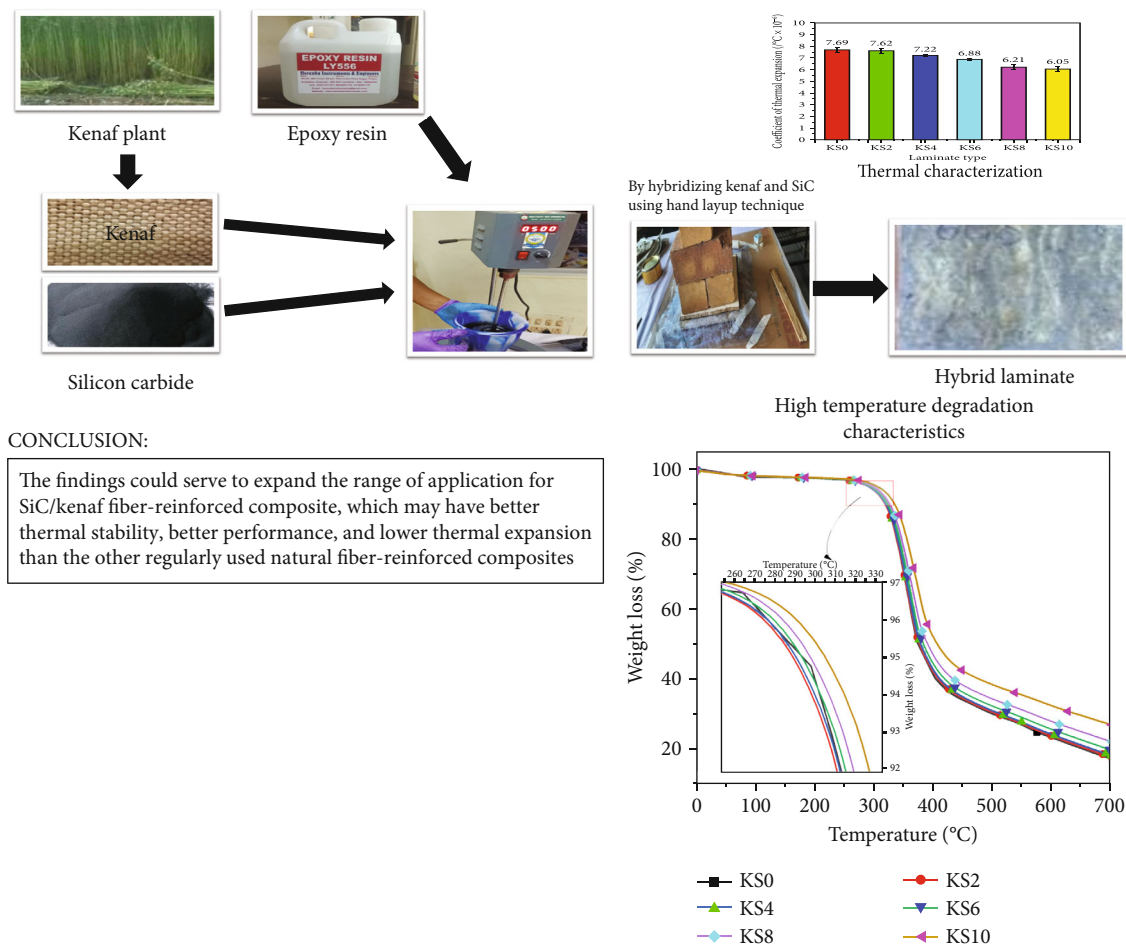


FIGURE 1: Methodology.

out for 24 hours. Void fraction in the composite laminates was reduced in the rate of 0.16 reduction per 2% SiC added. Total void reduction percentage is 98.9% by adding 10% SiC (KS10 laminate). Then, the laminates were trimmed according to ASTM standards after being removed from the mold for various tests to be performed. Tables 2 and 3 illustrate calculations on reinforcement fraction and void fraction, respectively.

4. Experimentation

The thermal conductivity was determined using ASTM E-1530 at a temperature of 55°C. The test was conducted using a guarded hot plate instrument. The thermal conductivity test used 50 mm × 50 mm specimen size as a reference [28]. With the dimensions of 127 mm × 12.7 mm and a dilatometer device, CTE is measured according to ASTM D696-08e1. A displacement sensor attached to the end of the pushrod measures the increase in length of the specimen, while it is heated in a furnace [29]. The heat deflection temperature of composite laminates was obtained using the Presto HDT/VSP Tester in a three-point bending method according to ASTM D648. The HDT was measured for each specimen under 1.5 MPa stress at a 0.25 mm deflection and a 2°C/minute heating rate [30]. EXSTAR TG/DTA 6300, Hita-

chi, Japan, is used to do thermographic analysis. The equipment has a temperature accuracy of 5°C. 10 mg of powdered samples was put in a 7 mm diameter alumina crucible. With 50 cm³/min nitrogen flow, the specimen was heated at a 10°C/min rate from 50°C to 600°C. The data acquired was shown as TG curve (weight loss as a function of temperature) and DTG curve (Derivative Thermogravimetric), the weight loss rate as a function of temperature [31]. Using a DSC Q20 from TA Instruments, DSC analysis was used to quantify changes in heat flows associated with material transitions in composites. Under nitrogen air, a sample weighing 3–4 mg was heated at a rate of 10°C/min from 25 to 350°C in an aluminum crucible with a pinhole. Each composition had three samples analyzed. Each fiber sample was examined independently before being compared [32]. Thermal property tests such as HDT, CTE, and thermal conductivity tests conducted were repeated with three specimens each, and standard deviations are included.

5. Result and Discussion

5.1. Thermal Conductivity. Figure 2 showed the thermal conductivity pattern as in the form of an increase in %vol of SiC. The thermal conductivity of laminates is in the sequence of KS0 < KS2 < KS4 < KS6 < KS8 < KS10. It is observed from

TABLE 2: Calculation on reinforcement fraction.

S. no	Material code	Stacking sequences	Weight of composite	Weight of Kenaf fiber	Weight of silicon carbide fillers	Weight of matrix	Reinforcement volume fraction
			W_C	W_K	W_S	W_M	f_R
1	KS0	KFRP with no SiC fillers	297	119	0	178	0.354
2	KS2	KFRP with 2 vol% SiC fillers	322	119	25	178	0.374
3	KS4	KFRP with 4 vol% SiC fillers	348	119	51	178	0.394
4	KS6	KFRP with 6 vol% SiC fillers	378	119	81	178	0.416
5	KS8	KFRP with 8 vol% SiC fillers	406	119	110	178	0.435
6	KS10	KFRP with 10 vol% SiC fillers	438	119	142	178	0.455

TABLE 3: Calculation on void fraction and thickness of composites.

S.no	Material code	Actual density of composite	Theoretical density of composite	Void fraction	Thickness of composite
		ρ_{ac}	ρ_{tc}	f_v	T_C
1	KS0	1.04	1.24	0.273	4.56
2	KS2	1.15	1.3	0.146	4.48
3	KS4	1.280607	1.36	0.06	4.352
4	KS6	1.39	1.426	0.022	4.336
5	KS8	1.46	1.48	0.010	4.432
6	KS10	1.53	1.54	0.003	4.56

Figure 2 that the increase in silicon carbide fillers in polymers enhances its thermal conductivity. The laminate KS10, which has 10 percent of silicon carbide, has exhibited excellent thermal conductivity than the other laminates. KS10 laminate has a thermal conductivity of 0.713 W/mK which is 97.2% higher than the thermal conductivity of the laminate KS0 (0.36 W/mK). Molecular movement increases with an increase in temperature. Molecular movement is in high rate leads to the material's high thermal conductivity [33]. In the case of SiC, molecular movement is high, and thus, it produces high thermal conductivity [34]. High thermal conductive SiC fillers made the composite laminate have good thermal conductivity. Incorporating SiC fillers into composites is a good way to improve thermal conductivity. The high aspect ratio of SiC is also the reason for enhancing thermal conductivity [35]. The interaction between silicon carbide-filled matrix and treated kenaf fibers was good, and it made intermolecular mobility to transfer heat easier. Another factor is the well-dispersed SiC that makes a good network among them. The other composite KS2, KS4, KS6, and KS8 laminates exhibited thermal conductivity of 0.37, 0.41, 0.48, and 0.58 W/mK, respectively. From four volume percentage of SiC loading, the thermal conductivity enhanced considerably by 27.27% compared to that of KS2. Additionally, SiC loading is raised from 4% to

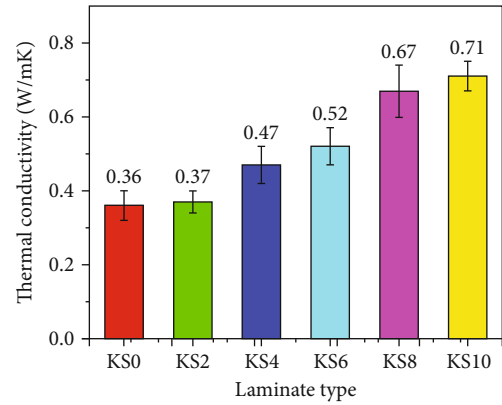


FIGURE 2: Thermal conductivity of composites.

8%. There is a substantial rise in thermal conductivity. Because of its poor crystallinity, KS0 cannot achieve the desired thermal conductivity.

5.2. Coefficient of Thermal Expansion. The thermal expansion coefficient decreases with adding fillers in the composite. Silicon carbide is an important filler because of its strong bond between atoms, resulting in low CTE [36, 37]. When silicon carbide is added to the composite, it reduces the CTE of the composite. It is also agreed with Nadh et al. [38]. The interaction of the epoxy chains with SiC causes the emergence of limitations to their motions [39]. The SiC scattered in the matrix could be used as a scaffold to successfully regulate the polymer chain movement. From Figure 3, it is observed that the laminate KS0 performed a higher coefficient of thermal expansion (CTE) over other laminates. The coefficient of thermal expansion increases with an increase in SiC fillers, in the composite. The lower thermal strain in SiC-filled composite leads to a poor coefficient of thermal expansion (CTE) [40]. The laminate KS10 produced a lower CTE value of $6.05 \times 10^{-6}/^{\circ}\text{C}$, which is 21.32% lower than the CTE of KS0 laminate ($7.69 \times 10^{-6}/^{\circ}\text{C}$). The KS2, KS4, KS6, and KS8 laminates also

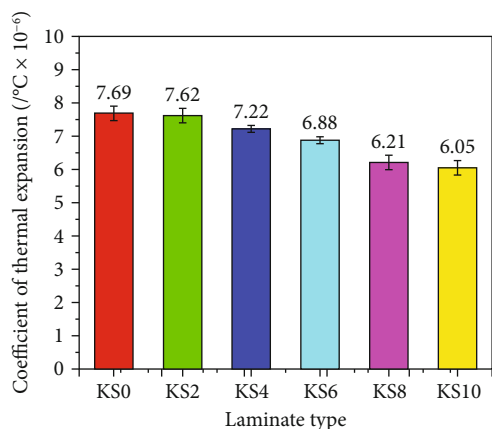


FIGURE 3: Coefficient of thermal expansion of composites.

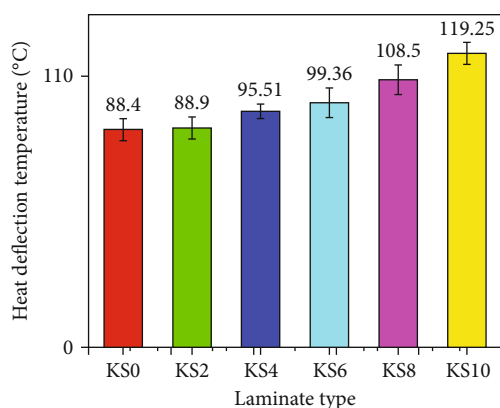


FIGURE 4: Heat deflection temperature of composites.

have lower CTE than KS0. The CTE values of laminates is in the order of $\text{KS0} > \text{KS2} > \text{KS4} > \text{KS6} > \text{KS8} > \text{KS10}$, in spite of an increase in SiC filler loading. The coefficient of thermal expansion of silicon carbide is $4.0 \times 10^{-6}/^{\circ}\text{C}$, which is lower than that of epoxy resin and kenaf fiber-reinforced epoxy composite (KS0)'s CTE ($45 - 55 \times 10^{-6}/^{\circ}\text{C}$ and $7.69 \times 10^{-6}/^{\circ}\text{C}$, respectively). When adding every 2% SiC into the kenaf fiber-reinforced composite, it decreases the CTE in an average rate of $0.328 \times 10^{-6}/^{\circ}\text{C}$ per 2% SiC addition in the composite. This result suggests that the inclusion of silicon carbide considerably reduces thermal expansion. This silicon carbide-filled natural fiber composites discovered potential application in structural materials.

5.3. Heat Deflection Temperature. HDT indicates how the composite responds when stressed at an elevated temperature. Dispersion levels of fibers and fillers, the crystallinity of materials, and the volume of fillers affect heat deflection temperature. An increase in silicon carbide fillers leads to an increase in heat deflection temperature of laminates. The laminate KS10 has a HDT of 119.25°C , which is 34.89% higher than the KS0 laminate. Since the thermal stability of silicon carbide is high, the composite with silicon carbide fillers is also high. Hence, an increase in silicon carbide content increases the HDT of the composite. The plas-

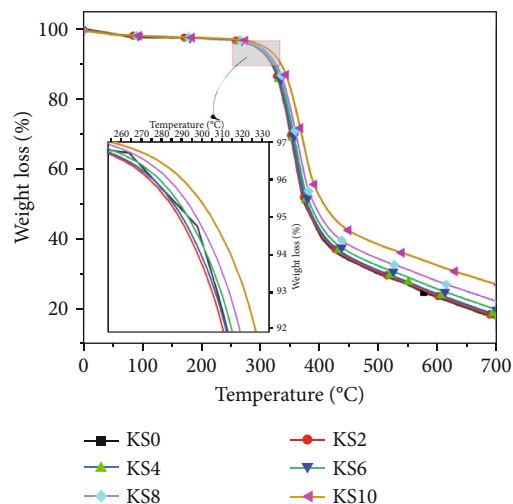


FIGURE 5: Thermogravimetric analysis of laminates (TGA).

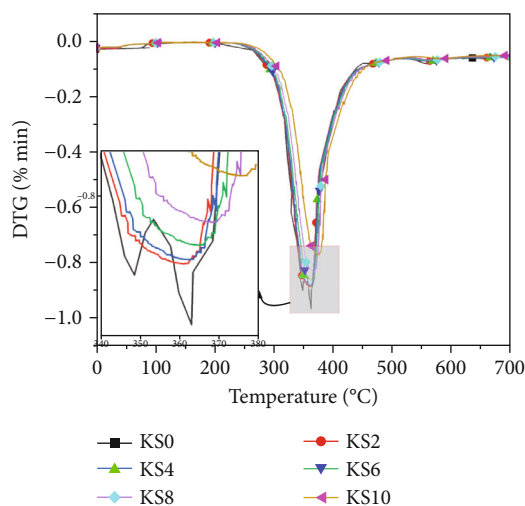


FIGURE 6: Derivative thermogravimetric analysis (DTG) of composites.

ticity decrement is also the reason for higher HDT. The plasticity of the composite decreased when introducing filler content in the materials. From Figure 4, significant rise in heat deflection temperature at the four vol% of silicon carbide in the composite can be noted. The HDT of 4 vol% KS4 laminate is 7.54% higher than 2 vol% KS2 laminate. Moreover, heat deflection temperature is increased in the order of $\text{KS0} < \text{KS2} < \text{KS4} < \text{KS6} < \text{KS8} < \text{KS10}$.

5.4. Thermogravimetric Analysis (TGA). TGA is used to analyze the performance of composite in terms of weight loss with increasing temperature characterization. Figures 5 and 6 show the TG and DTG curves of TGA carried out in the nitrogen atmosphere at $20^{\circ}\text{C}/\text{min}$ heating rate of different composite laminates. The initial DTG peak at $65-70^{\circ}\text{C}$ of laminates was associated with the loss of moisture content in the laminates. The hemicellulose decomposition peak for the uncontaminated fiber composite with no fillers (KS0) at 361°C was

TABLE 4: Weight loss and degradation temperatures of composites.

S. no.	Laminate type	Weight percentage		Total weight loss percentage	T onset	Tmax	% Residue at 700
		At 250	At 500				
1	KS0	96.68	28.95	67.73	302.66	361	17.06
2	KS2	96.74	30.6	66.14	314.18	361.51	17.71
3	KS4	96.78	30.95	65.83	319.81	362.99	18.2
4	KS6	96.88	32.29	64.59	322.38	364.59	19.364
5	KS8	96.97	34.95	62.02	325.11	368.87	22.16
6	KS10	97.04	38.43	58.61	331.65	377.44	24.93

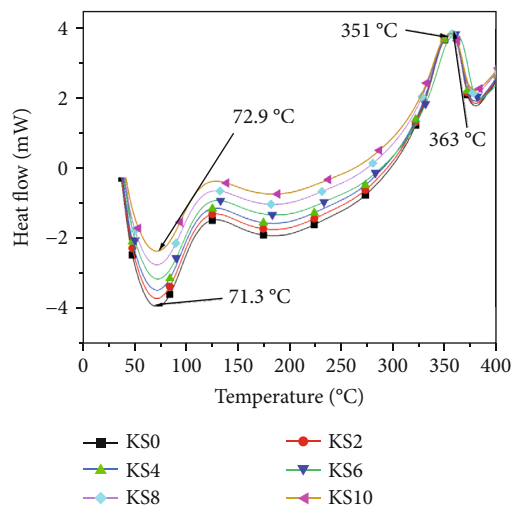


FIGURE 7: Differential scanning calorimetry (DSC) curves of composites.

observed from the DTG curve of KS0 laminate. From the TG curve of KS0 laminate, 50% weight loss of KS0 laminate was observed at 378°C. 67.73% of mass loss over the temperature range of 250°C to 500°C in KS0 laminate could be observed. This mass loss could be attributed to lignin, hemicellulose, cellulose, and depolymerization of polymers. Specifically, from the DTG curve, the peak at 50°C is associated with loss of moisture, solvents, and volatile contents present in the composite, whereas the peak at 361°C is attributed to the loss of cellulose and hemicelluloses present in the composite and further at around 500 363°C is associated with loss of lignin content in the composite [41].

Similarly, it could be noted that from the TG curves of KS2, KS4, KS6, KS8, and KS10 laminates, percentage mass loss over the temperature range of 250°C to 500°C is 66.14, 65.83, 64.59, 62.02, and 58.61, respectively. As for the DTG curve, over the temperature range 250°C to 500°C, the peaks of KS2, KS4, KS6, KS8, and KS10 laminates are 361.51°C, 362.99°C, 364.59°C, 368.87°C, and 377.44°C, respectively. Observations made from the TG and DTG curves indicated that the inclusion of silicon carbide fillers delayed the rate of mass loss and mass loss percentages over the temperature range of 250°C to 500°C and also indicated no loss or gain due to the addition of SiC fillers in the laminates which reveals that silicon carbide did not react with any element present in the laminates over the temperature ranges and at nitrogen atmosphere.

Figures 5 and 6 showed TG/DTG curves obtained for laminates. The first stage (25°C to 150°C) of curves indicated that loss of mass decreases with an increase in silicon carbide fillers since fillers and epoxy resins are hydrophobic in nature and replace fiber contents. It indicated that the volatile component and moisture content present in the composite materials are low as an increase in SiC fillers. TGA parameters such as onset degradation temperature, maximum degradation temperature, mass loss percentage, and residues were listed in Table 4. The predicted point of departure from the initial slope, practically a horizontal line in TG curves, was used to determine the commencement of thermal deterioration (T onset). maximum degradation temperature (Tmax) was obtained from DTG peaks attributed to the maximum mass loss rate in the steeper region of the DTG curve between 100°C and 500°C.

The onset temperature of KS0 laminate was around 302.66°C, whereas the onset temperature of the KS10 laminate was around 331.65°C. The T onset of other laminates such as KS2, KS4, KS6, and KS8 are 314.18°C, 319.81°C, 322.38°C, and 325.11°C, respectively. It was discovered that when the amount of SiC fillers in a composite rises, the temperature at which it begins to degrade increases. Natural fiber-reinforced polymers are thought to have a safe operating temperature of roughly 300°C [41]. For the SiC-reinforced kenaf fiber composite, the maximum safe working temperature eventually increased to 330°C.

It is worth observing that increasing the SiC fillers in the composites attributed to the thermal stabilization of material. It is ratified by a rise in residue contents of composites at 700°C, mainly KS10 laminate, whereas for KS0 laminate, there is a small quantity of char residue at 700°C. The residues for KS2, KS4, KS6, and KS8 laminates are 17.71%, 18.2%, 19.36%, and 22.16%, respectively. The results indicate that increasing SiC filler increases the char residue percentage and thermal stabilization accordingly. The reason for enhancement in thermal stability is SiC filler interactions with the composite which is delaying the degradation temperature of the composites.

5.5. Differential Scanning Calorimetry (DSC). Samples of fabricated composite laminates were investigated in detail using differential scanning calorimetry. From Figure 7, the DSC curve of the KS0 sample showed an endothermic peak at the temperature of 70.09°C attributed to moisture content loss from the sample. Furthermore, endothermic peaks for the KS2, KS4, KS6, KS8, and KS10 samples are at temperatures

71.3°C, 71.9°C, 72.2°C, 72.5°C, and 72.9°C, respectively. It is clearly noticed that the loss of moisture and volatiles present in the samples were low and thermal stability of composite was high with the increase in SiC fillers. Glass transition temperature (T_g) is highly dependent on the mobility of the polymer chain [42]. Addition of filler materials and plasticizers increases the glass transition temperature, and it reduces the mobility of polymer chain [43].

Decomposition of cellulose in the samples was observed at the temperature; the exothermic peaks for all samples were residing between 351°C and 363°C. It is clearly observed that the heat flow over the sample increases with an increase in SiC fillers. Moreover, the exothermic peak of the KS10 sample was obtained at 363°C which was 41% higher than the temperature observed in the KS0 sample. The results revealed that the thermal stability of the composite improved as the quantity of SiC in the composite increased. The exothermic peaks of specimens attributed to loss of lignin and cellulose in the specimens [26]. The glass transition temperature of the samples was obtained between 50°C and 55°C with a consecutive increase in SiC fillers in the composite. It evidently observed that the addition of SiC particles in hybrids delayed the glass transition. SiC fillers did not undergo any chemical changes in the N₂ atmosphere at a higher temperature of 700°C. It is noted from the DSC curves of samples by observing that the curves had no peaks due to the presence of SiC fillers.

6. Conclusion

The thermal characteristics of silicon carbide/kenaf fiber-reinforced epoxy composites with different weight percentages were studied. Six different composite specimens were fabricated at varying weight percentages of silicon carbide. The specimens were subjected to various thermal tests, such as heat deflection temperature, coefficient of thermal expansion, thermal conductivity, thermogravimetric analysis (TGA), and differential scanning calorimetry (DSC).

The thermal conductivity of kenaf fiber polymer hybrids with 10 vol% of SiC is 0.71 W/mK, which is 97.22% higher than that of pure kenaf fiber composite (0.36 W/mK). The inclusion of SiC to hybrids improves their thermal conductivity.

The CTE of the hybrids with 10% of SiC was $6.05 \times 106/^\circ\text{C}$, which is 21.32 percent less than the CTE of the pure kenaf fiber-reinforced composite ($7.69 \times 106/^\circ\text{C}$). CTE is also lower in hybrids with 2%, 4%, 6%, and 8% of SiC than in pure kenaf fiber-reinforced composite.

The HDT of the KS10 laminate is 119.25°C, which is 34.89 percent greater than the HDT of the KS0 laminate. Because silicon carbide had high thermal stability, the composite with silicon carbide fillers has high thermal stability as well. As a result, increasing the silicon carbide content raises the composite's heat deflection temperature.

The results of TGA and DSC analysis revealed that the increase in SiC fillers in the kenaf fiber-reinforced polymers enhanced the thermal stability of hybrid polymers. The temperature at which a material begins to decompose and the extent of mass change assessed by thermogravimetry are

both considered to be thermal stability. This temperature might represent the material's maximum working temperature in structural applications. The highest safe working temperature of the SiC/kenaf fiber-reinforced composite was observed at 330°C.

With more SiC filler in the hybrids, the weight loss % between 250°C and 500°C was reduced. The onset degradation temperature and residues at 700°C were increased with an increase in SiC fillers in the hybrids. Residues at 700°C of hybrid with 10% SiC was 22.16% higher than the composite with no SiC fillers. According to the DSC study, the glass transition temperature and the temperature at which lignin and cellulose degradation occurred increased with the increase in SiC nanoparticles.

These findings could serve to expand the range of application for SiC/kenaf fiber-reinforced composite, which may have better thermal stability, better performance, and lower thermal expansion than the other regularly used natural fiber-reinforced composites. Automotive interior parts are made of polypropylene (PP), acrylonitrile-butadiene-styrene (ABS), and styrene maleic anhydride (SMA) materials. The materials mentioned above have the maximum heat deflection temperature of around 70°C. The present study results indicated better strength than the commercially used automobile interior parts. Heat deflection temperature of composite KS10 is 70.35% higher than that of industrial materials utilized in automotive interior parts.

Data Availability

The data used to support the findings of this study are included in the article. Should further data or information be required, these are available from the corresponding author upon request.

Conflicts of Interest

The authors declare that there are no conflicts of interest regarding the publication of this paper.

Acknowledgments

The authors thank the Vel Tech Rangarajan Dr. Sagunthala R&D Institute of Science and Technology, Chennai, for providing characterization support to complete this research work.

References

- [1] K. P. Ashik and R. S. Sharma, "A review on mechanical properties of natural fiber reinforced hybrid polymer composites," *Journal of Minerals and Materials Characterization and Engineering*, vol. 3, no. 5, pp. 420–426, 2015.
- [2] H. Abdellaoui, M. Raji, R. Bouhfid, and A. el Kacem Quaiss, "2-investigation of the deformation behavior of epoxy-based composite materials," in *Fail. Anal. Biocomposites Fibre-Reinf. Compos. Hybrid Compos.*, M. Jawaid, M. Thariq, and N. Saba, Eds., pp. 29–49, Woodhead Publishing, 2019.
- [3] V. Paranthaman, K. S. Sundaram, and L. Natrayan, "Effect of silica content on mechanical and microstructure behaviour

- of resistance spot welded advanced automotive trip steels,” *SILICON*, vol. 14, pp. 1–10, 2021.
- [4] T. Rohan, B. Tushar, and G. T. Mahesha, “Review of natural fiber composites,” in *IOP Conference Series: Materials Science and Engineering*, vol. 314, IOP Publishing, p. 012020, 2018.
 - [5] Y. Sesharao, T. Sathish, K. Palani, A. Merneedi, M. V. De Pours, and T. Maridurai, “Optimization on operation parameters in reinforced metal matrix of AA6066 composite with HSS and Cu,” *Advances in Materials Science and Engineering*, vol. 2021, Article ID 1609769, 12 pages, 2021.
 - [6] M. Chandrasekar, M. R. Ishak, S. M. Sapuan, Z. Leman, and M. Jawaid, “A review on the characterisation of natural fibres and their composites after alkali treatment and water absorption,” *Plastics, Rubber and Composites*, vol. 46, no. 3, pp. 119–136, 2017.
 - [7] P. Anand, D. Rajesh, M. Senthil Kumar, and I. Saran Raj, “Investigations on the performances of treated jute/Kenaf hybrid natural fiber reinforced epoxy composite,” *Journal of Polymer Research*, vol. 25, no. 4, 2018.
 - [8] M. R. Nurul Fazita, M. J. Nurnadia, H. P. S. Abdul Khalil, M. K. Mohamad Haafiz, H. M. Fizree, and N. L. M. Suraya, “Woven natural fiber fabric reinforced biodegradable composite: processing, properties and application,” in *Green Biocomposites Manuf. Prop.*, M. Jawaid, S. M. Sapuan, and O. Y. Alothman, Eds., pp. 199–224, Springer International Publishing, Cham, 2017.
 - [9] H. M. Akil, M. F. Omar, A. A. M. Mazuki, S. Safiee, Z. A. M. Ishak, and A. A. Bakar, “Kenaf fiber reinforced composites: a review,” *Materials and Design*, vol. 32, no. 8-9, pp. 4107–4121, 2011.
 - [10] L. Natrayan, R. Anand, and S. Santhosh Kumar, “Optimization of process parameters in TIG welding of AISI 4140 stainless steel using Taguchi technique,” *Materials Today: Proceedings*, vol. 37, pp. 1550–1553, 2021.
 - [11] K. Malik, F. Ahmad, and E. Gunister, “A review on the kenaf fiber reinforced thermoset composites,” *Applied Composite Materials*, vol. 28, no. 2, pp. 491–528, 2021.
 - [12] P. Asha, L. Natrayan, B. T. Geetha et al., “IoT enabled environmental toxicology for air pollution monitoring using AI techniques,” *Environmental Research*, vol. 205, p. 112574, 2022.
 - [13] M. S. K. Sharma, S. Umadevi, Y. S. Sampath et al., “Mechanical behavior of silica fume concrete filled with steel tubular composite column,” *Advances in Materials Science and Engineering*, vol. 2021, Article ID 3632991, 9 pages, 2021.
 - [14] A. Alavudeen, N. Rajini, S. Karthikeyan, M. Thiruchitrabalam, and N. Venkateshwaren, “Mechanical properties of banana/kenaf fiber-reinforced hybrid polyester composites: effect of woven fabric and random orientation,” *Materials & Design (1980-2015)*, vol. 66, pp. 246–257, 2015.
 - [15] G. R. Arpitha, M. R. Sanjay, P. Senthamaraiannan, C. Barile, and B. Yogesha, “Hybridization effect of sisal/glass/epoxy/filler based woven fabric reinforced composites,” *Experimental Techniques*, vol. 41, no. 6, pp. 577–584, 2017.
 - [16] K. Srinivas and M. S. Bhagyashekar, “Thermal conductivity enhancement of epoxy by hybrid particulate fillers of graphite and silicon carbide,” *Journal of Minerals and Materials Characterization and Engineering*, vol. 3, no. 2, pp. 76–84, 2015.
 - [17] W. Cheewawuttipong, D. Fuoka, S. Tanoue, H. Uematsu, and Y. Iemoto, “Thermal and mechanical properties of polypropylene/boron nitride composites,” *Energy Procedia*, vol. 34, pp. 808–817, 2013.
 - [18] S. N. Monteiro, V. Calado, R. J. S. Rodriguez, and F. M. Margem, “Thermogravimetric behavior of natural fibers reinforced polymer composites—an overview,” *Materials Science and Engineering A*, vol. 557, pp. 17–28, 2012.
 - [19] N. Jesuarockiam, M. Jawaid, E. S. Zainudin, M. T. Hameed Sultan, and R. Yahaya, “Enhanced thermal and dynamic mechanical properties of synthetic/natural hybrid composites with graphene nanoplatelets,” *Polymers*, vol. 11, no. 7, p. 1085, 2019.
 - [20] A. Merneedi, N. Mohan Rao, L. Natrayan, L. Yuvaraj, and P. Paramasivam, “Free vibration analysis of thick rectangular and elliptical plates with concentric cut-out,” *Advances in Materials Science and Engineering*, vol. 2021, Article ID 7212075, 14 pages, 2021.
 - [21] K. Liu, X. Zhang, H. Takagi, Z. Yang, and D. Wang, “Effect of chemical treatments on transverse thermal conductivity of unidirectional abaca fiber/epoxy composite,” *Composites. Part A, Applied Science and Manufacturing*, vol. 66, pp. 227–236, 2014.
 - [22] S. Madupalli, K. Vasugi, and R. Kumar, “Structural performance of non-linear analysis of turbo generator building using seismic protection techniques,” *International Journal of Recent Technology and Engineering*, vol. 8, no. 1, pp. 1091–1095, 2019.
 - [23] S. D. Salman, M. J. Sharba, Z. Leman, M. T. H. Sultan, M. R. Ishak, and F. Cardona, “Physical, mechanical, and morphological properties of woven kenaf/polymer composites produced using a vacuum infusion technique,” *International Journal of Polymer Science*, vol. 2015, Article ID 894565, 10 pages, 2015.
 - [24] “Silicon Carbide SiC Material Properties,” February 2022 <http://accuratus.com/silicar.html>.
 - [25] M. Meikandan, K. Malarmohan, and R. Velraj, “Development of superhydrophobic surface through facile dip coating method,” *Digest Journal of Nanomaterials and Biostructures*, vol. 11, pp. 945–951, 2017.
 - [26] M. Meikandan, M. Sundarraj, D. Yogaraj, and K. Malarmohan, “Experimental and numerical investigation on bare tube cross flow heat exchanger-using COMSOL,” *International Journal of Ambient Energy*, vol. 41, no. 5, pp. 500–510, 2020.
 - [27] M. Vijayaragavan, B. Subramanian, S. Sudhakar, and L. Natrayan, “Effect of induction on exhaust gas recirculation and hydrogen gas in compression ignition engine with simarouba oil in dual fuel mode,” *International Journal of Hydrogen Energy*, vol. 47, pp. 1–13, 2021.
 - [28] R. C. Mohapatra, “Experimental study on optimization of thermal properties of natural fibre reinforcement polymer composites, open access,” *Library Journal*, vol. 5, pp. 1–15, 2018.
 - [29] D. L. Motoc, J. Ivens, and N. Dadirlat, “Coefficient of thermal expansion evolution for cryogenic preconditioned hybrid carbon fiber/glass fiber-reinforced polymeric composite materials,” *Journal of Thermal Analysis and Calorimetry*, vol. 112, no. 3, pp. 1245–1251, 2013.
 - [30] N. D. K. R. Chukka, L. Natrayan, and W. D. Mammo, “Seismic fragility and life cycle cost analysis of reinforced concrete structures with a hybrid damper,” *Advances in Civil Engineering*, vol. 2021, Article ID 4195161, 17 pages, 2021.
 - [31] M. Meikandan and K. Malarmohan, “Fabrication of a superhydrophobic nanofibres by electrospinning,” *Digest Journal of Nanomaterials & Biostructures*, vol. 12, no. 1, pp. 11–17, 2017.

- [32] H. A. Aisyah, M. T. Paridah, S. M. Sapuan et al., "Thermal properties of woven kenaf/carbon fibre-reinforced epoxy hybrid composite panels," *International Journal of Polymer Science*, vol. 2019, Article ID 5258621, 8 pages, 2019.
- [33] S. Kumar, A. Saha, and S. Bhowmik, "Accelerated weathering effects on mechanical, thermal and viscoelastic properties of kenaf/pineapple biocomposite laminates for load bearing structural applications," *Journal of Applied Polymer Science*, vol. 139, no. 2, p. 51465, 2022.
- [34] R. Chaturvedi, A. Pappu, P. Tyagi et al., "Next-generation high-performance sustainable hybrid composite materials from silica-rich granite waste particulates and jute textile fibres in epoxy resin," *Industrial Crops and Products*, vol. 177, p. 114527, 2022.
- [35] C. S. S. Anupama, L. Natrayan, E. Laxmi Lydia et al., "Deep learning with backtracking search optimization-based skin lesion diagnosis model," *Computers, Materials & Continua*, vol. 70, no. 1, pp. 1297–1313, 2022.
- [36] T. B. Asafa, M. O. Durowoju, K. P. Madingwaneng et al., "Gr-Al composite reinforced with Si₃N₄ and SiC particles for enhanced microhardness and reduced thermal expansion," *SN Applied Sciences*, vol. 2, no. 6, pp. 1–12, 2020.
- [37] Y. Wang, J. Wu, Y. Yin, and T. Han, "Effect of micro and nano-size boron nitride and silicon carbide on thermal properties and partial discharge resistance of silicone elastomer composite," *IEEE Transactions on Dielectrics and Electrical Insulation*, vol. 27, no. 2, pp. 377–385, 2020.
- [38] V. S. Nadh, C. Krishna, L. Natrayan et al., "Structural behavior of nanocoated oil palm shell as coarse aggregate in lightweight concrete," *Journal of Nanomaterials*, vol. 2021, Article ID 4741296, 7 pages, 2021.
- [39] S. Arul, M. Easwaramoorthi, and M. Meikandan, "Comparison of nano coated aluminum plate and nano coated copper plate for development of energy efficient heating/cooling system," *International Journal of Applied Engineering Research*, vol. 4, no. 4, 2014.
- [40] S. K. Park, J. I. Han, W. K. Kim, and M. G. Kwak, "Deposition of indium-tin-oxide films on polymer substrates for application in plastic-based flat panel displays," *Thin Solid Films*, vol. 397, no. 1-2, pp. 49–55, 2001.
- [41] K. Hemalatha, C. James, L. Natrayan, and V. Swamynadh, "Analysis of RCC T-beam and prestressed concrete box girder bridge's super structure under different span conditions," *Materials Today: Proceedings*, vol. 37, no. 2, pp. 1507–1516, 2021.
- [42] C. Lu, Q. Yuan, R. Simons et al., "Influence of SiC and VGCF nano-fillers on crystallization behaviour of PPS composites," *Journal of Nanoscience and Nanotechnology*, vol. 16, no. 8, pp. 8366–8373, 2016.
- [43] S. Rimdusit, V. Jiraprawatthagool, C. Jubsilp, S. Tiptipakorn, and T. Kitano, "Effect of SiC whisker on benzoxazine-epoxy-phenolic ternary systems: microwave curing and thermomechanical characteristics," *Journal of Applied Polymer Science*, vol. 105, no. 4, pp. 1968–1977, 2007.